Rotons and Quantum Evaporation from Superfluid ^{4}He

F. Dalfovo,[1] A. Fracchetti,[1] A. Lastri,[1] L. Pitaevskii,[1,2,3] and S. Stringari[1]
[1]*Dipartimento di Fisica, Università di Trento, and INFM, 38050 Povo, Italy*
[2]*Department of Physics, Technion, Haifa 32000, Israel*
[3]*Kapitza Institute for Physical Problems, 117334 Moscow, Russia*
(Received 26 May 1995)

The probability of evaporation induced by rotons at the surface of superfluid helium is calculated using time dependent density functional theory. We consider excitation energies and incident angles such that phonons do not take part in the scattering process. We predict sizable evaporation rates, which originate entirely from quantum effects. Results for the atomic reflectivity and for the probability of the roton change-mode reflection are also presented.

PACS numbers: 67.40.Db

Quantum evaporation occurs in superfluid ^{4}He when a high-energy phonon or roton propagates to the surface where it annihilates and an atom is ejected in the free space (see, for example, Ref [1]). This phenomenon is especially interesting because of the peculiar dispersion law exhibited by rotons.

Despite the significant experimental [2–8] and theoretical [9–14] efforts made in the last years, the fundamental mechanisms underlying the phenomenon of quantum evaporation are not yet understood. The experiments by Wyatt and co-workers [1,5,6] have revealed that the main process is a one to one process (one excitation to one atom). This behavior is confirmed by the separate conservation of the energy and of the momentum parallel to the surface in the evaporation process. Conversely measurements of atom condensation [15,16] point out an important role of nonlinear processes associated with the excitation of ripplons. This apparent asymmetry between evaporation and condensation processes is still unexplained (see Ref. [13] for a recent discussion).

The theoretical studies have not yet provided a clear and consistent picture of quantum evaporation. The reason is that it is very difficult to develop a reliable description of this phenomenon on a microscopic basis. In fact a good theory should be able to account for several effects: (i) a correct description of the structure of the free surface, as well as of the elementary excitations of the system; (ii) a quantum description of the scattering processes involving the elementary excitations at the surface; and (iii) the inclusion of inelastic channels (multiphonons, multiripplons).

A useful discussion concerning the role of quantum effects has been recently made in Refs. [13,14] where it has been pointed out that, due to the peculiar form of the maxon-roton dispersion exhibited by superfluid helium, there are severe constraints on the structure of the classical orbits associated with the elementary excitations when they cross the interface. In particular, one finds that only phonons and rotons above the maxon energy (about 14 K) can give rise to evaporation. Vice versa, the theory of classical orbits predicts no evaporation from rotons with energy smaller than the maxon energy, because of the occurrence of a barrier at the interface. The experimental evidence [1,5] for quantum evaporation induced by rotons even below the maxon energy is consequently an important proof of the crucial role played by quantum effects. The quantum states associated with the above classical orbits (WKB states) have been also used to carry out a perturbative description of the scattering process [14]. However, the perturbative approach is not easily justifiable in this context.

The purpose of this Letter is to provide a first calculation of the evaporation rates using a many body approach accounting for both the requirements (i) and (ii) discussed above.

As in Ref. [17] we work in a slab geometry (liquid between two parallel surfaces). The computation is done in a box of size $L_{\rm box}$, containing the slab. The system is assumed to be translationally invariant in the x, y direction, while z is orthogonal to the surfaces. The slab is chosen thick enough (50–70 Å) to provide a quantitatively correct description of the behavior of the semi-infinite medium. The box size ($L_{\rm box} > 100$ Å) has been chosen in order to allow a few oscillations of the atom wave function in the free space. The main features of the spectrum of the elementary excitations are shown in Fig. 1 as a function of q_x (for a more detailed discussion see Ref. [17]). For a given value of q_x one finds excitations propagating at different angles, i.e., different values of q_z. In particular, in the shaded area one finds rotons with negative and positive group velocity (R^- and R^+, respectively) with energy larger than the threshold for atom evaporation (dashed line). In this work we limit ourselves to this part of the spectrum where phonons do not take part in the scattering process because of energy and momentum conservation. It is worth mentioning that, according to the classical picture of Ref. [13], atoms traveling at incidence angles sufficiently large, so that they lie in the shaded area in Fig. 1, are reflected with unit probability. This behavior

 0031-9007/95/75(13)/2510(4)$06.00

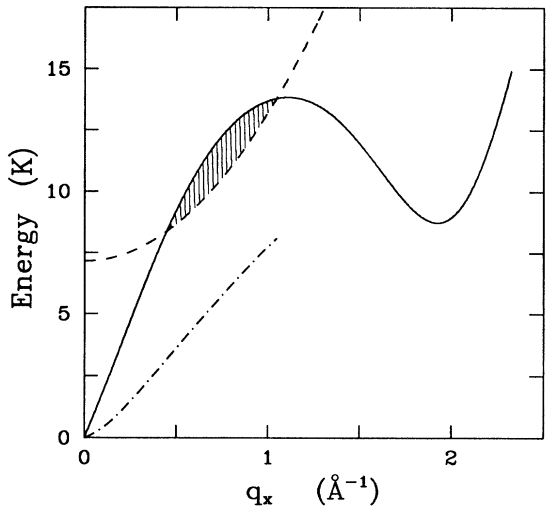

FIG. 1. Spectrum of elementary excitations. Solid line: phonon-roton dispersion in bulk liquid; dashed line: threshold for atom evaporation; dot-dashed line: dispersion of the surface mode; shaded area: region of roton-atom processes.

is contradicted by the experiments of Ref. [15], which instead indicate full condensation also in that region [18].

We have calculated the eigenenergies and eigenfunctions of this system in the framework of density functional theory, as already done in Refs. [17,19]. When applied to a Bose system this theory describes the fluctuations of the density ρ and of the velocity potential ϕ according to the expansion

$$\psi(\mathbf{r},t) \equiv \sqrt{\rho(\mathbf{r},t)}\, e^{i\phi(\mathbf{r},t)} = \psi_0(z) + f(z)e^{i(q_x x-\omega t)} + g(z)e^{i(q_x x+\omega t)}, \quad (1)$$

where $\psi_0(z) = \sqrt{\rho_0(z)}$ is fixed by the ground state density of the system and $f(z)$ and $g(z)$ are real wave functions to be determined, together with the frequency ω, by solving self-consistently the equations of motion

$$\delta \int dt \int d\mathbf{r}\left(\mathcal{H}[\psi^*,\psi] - \psi^* i\hbar \frac{\partial}{\partial t}\psi\right) = 0 \quad (2)$$

linearized with respect to f and g. The quantity $E = \int d\mathbf{r}\, \mathcal{H}[\psi^*,\psi]$ is the energy functional of the system (depending on ρ and ϕ) which is assumed to be known. The same functional provides, through the variational procedure $\delta(E - \mu N) = 0$, the ground state profile $\rho_0(z)$. In this work we use the density functional recently proposed in Ref. [19]. It provides an accurate description of the equation of state of superfluid helium, as well as of the density profile at the surface.

The density functional approach is basically a mean field theory with phenomenological ingredients fixed to reproduce known properties of the bulk liquid. We refer to Refs. [17,19] for a detailed discussion of the theory. Here we stress that Eqs. (1) and (2) have the typical form of the equations of the random phase approximation (RPA). In particular they account for both particle-hole $[f(z)]$ and hole-particle $[g(z)]$ transitions which are coupled by the equations of motion (2). This coupling is of crucial importance in order to treat the correlation effects associated with the propagation of elementary excitations in an interacting system. The equations of motion have also a structure formally identical to the one of the Bogoliubov equations for the dilute Bose gas and to the one of the Beliaev equations for Bose superfluids [14,20]. With respect to these theories the present approach makes use of a finite ranged and momentum dependent effective interaction, which allows one to reproduce the phonon-roton dispersion law. The same theory gives a reliable description of surface modes (ripplons) at both small and high momenta [17]. In the vacuum the equations of motion coincide with the Schrödinger equation for the free atom wave function $f(z)$, while $g(z)$ vanishes.

One should note that the equations of time dependent density functional (TDDF) theory correspond to quantum mechanical equations and consequently account for the interference and tunneling phenomena which are expected to play a crucial role in the evaporation process. Of course, due to linearization, they do not include inelastic processes associated with multiphonons or multiripplons. These effects lie beyond the present theory. Despite the absence of inelastic processes, we think that the solution of the evaporation problem within linearized TDDF theory is nevertheless highly instructive.

The solution of Eq. (2) can be determined with high precision working in the slab geometry discussed above. The solutions are real and either symmetric or antisymmetric with respect to the center of the slab. A typical solution is shown in Fig. 2(a), where we plot the function $f(z)$, for an excitation at $q_x = 0.7$ Å^{-1} and $\hbar\omega = 11$ K. The figure shows the existence of atoms traveling outside the slab and of elementary excitations inside the slab. The corresponding function $g(z)$, not shown, has also an oscillatory behavior inside the slab, while it vanishes outside consistently with the fact that the hole-particle components of the wave function (1) (associated with correlation effects) are absent in the free atom region. The wavelength of the atom wave function along z is easily calculated starting from the energy conservation law $\hbar\omega = \hbar^2 q^2/2m - \mu$ where $q^2 = q_x^2 + q_z^2$, while $\mu = -7.15$ K is the chemical potential of helium atoms. One finds $\lambda_z = 2\pi/q_z = 16.4$ Å in agreement with the numerical results shown in Fig. 2(a). With these values of q_x and q_z, the incident angle for the atom is about 61°.

Because of the values of q_x and ω the solution shown in Fig. 2(a) cannot contain phonon components. This is best illustrated in Fig. 2(b) where we show the Fourier transform of the signal inside the slab. The signal reveals two distinct peaks, one corresponding to a R^- roton with $q_z = 1.43$ Å^{-1} ($q = 1.59$ Å^{-1}), and the other to a R^+

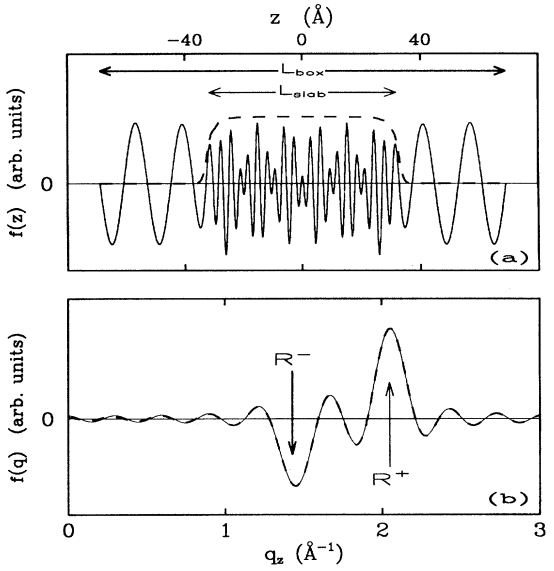

FIG. 2. An example of solution $f(z)$ for $q_x = 0.7$ Å^{-1}, $\hbar\omega = 11$ K, $L_{\rm slab} = 62$ Å, and $L_{\rm box} = 140$ Å. The dashed line in (a) is the density profile of the slab, in arbitrary units. In (b) the Fourier transform of $f(z)$ inside the slab is also shown. The best fit with formula (3) (dashed line) is practically indistinguishable from the numerical solution (solid line).

roton with $q_z = 2.05$ Å^{-1} ($q = 2.17$ $^{-1}$). In this case the R^- and R^+ rotons propagate at angles of 26° and 19° relative to the z axis, respectively. The additional oscillatory structure revealed by Fig. 2(b) originates from the finite size of the box, smaller than $L_{\rm slab}$, used to calculate the Fourier transform. In fact one can well fit the calculated signal starting from a function of the form

$$f(z) = f_+ \cos(q_z^+ z) + f_- \cos(q_z^- z) \qquad (3)$$

inside the slab and $f(z) = 0$ outside, as shown in Fig. 2(b). Actually this fitting procedure has been used in order to extract the values of f_+ and f^- needed for the analysis of the evaporation rates. The same procedure has been used to analyze the function $g(z)$.

The results for f and g can be used to calculate the current giving the number of elementary excitations crossing the unit surface per unit time through the following equation:

$$\mathbf{j}_i = \mathbf{v}_i(|f_i|^2 - |g_i|^2), \qquad (4)$$

where $|f_i|^2 - |g_i|^2$ is the density of elementary excitations and $\mathbf{v}_i$ is the group velocity of the ith excitation ($i = a, +, -$). The structure of the current (4) emphasizes a remarkable feature of the RPA (or Bogoliubov) equations. Note that only for a free atom Eq. (4) takes the familiar form $\mathbf{j} = |f|^2\hbar\mathbf{q}/m$. In a correlated system, like superfluid helium, the current behaves quite differently. For instance, in the long wavelength phonon regime ($q \longrightarrow 0$), the group velocity coincides with the sound velocity and $g \simeq f$.

The current (4) is used to calculate the (real) amplitudes $A_i = \sqrt{|j_i^z|}\,\mathrm{sgn}(f_i)$ of the signal relative to the various components (atom, $R^\pm$ rotons) in the scattering process taking place at the surface. The amplitude A_a of the signal relative to the outcoming atom can be related to the ones of the incoming atom and $R^\pm$ rotons through the relation

$$-A_a e^{-iq_z^a L_a} = S_{aa}A_a e^{iq_z^a L_a} + iS_{-a}A_- e^{-iq_z^- L} + iS_{+a}A_+ e^{iq_z^+ L}, \qquad (5)$$

where S_{ij} is the scattering matrix, $2L = L_{\rm slab}$ is the slab thickness, and $L_a = (L_{\rm box} - L_{\rm slab})/2$. Relation (5) holds for symmetric states; a similar relation can be written for antisymmetric states. Notice that the phonon contribution to the scattering process is absent due to the choice made for q_x and for the energy.

The matrix elements of the scattering matrix entering Eq. (5) satisfy the relation $S_{ij} = S_{ji}$ which follows from unitarity and time reversal symmetry conditions. In terms of these matrix elements the evaporation probabilities P^+ and P^- (relative to R^+ and R^- rotons) and the reflection coefficient R take the form

$$P^+ = |S_{+a}|^2\,, \qquad P^- = |S_{-a}|^2\,, \qquad R = |S_{aa}|^2\,. \qquad (6)$$

Furthermore, due to unitarity, one has $P^+ + P^- + R = 1$ (this is true only if one ignores inelastic channels, as in the present theory).

In order to extract the physical coefficients P^+, P^-, and R it is necessary to obtain various solutions at the same values of q_x and energy, involving different combinations of the atom and roton signals. This has been achieved by varying the thickness of the slab and the size of the box. Of particular importance, for our analysis, is the occurrence of the so-called "resonance" states which are characterized by the absence of the atom signal ($A_a = 0$) outside the slab, due to destructive interference. These states are useful because, as Eqs. (5) and (6) clearly show, they allow one to identify the ratio P^+/P^- with $|A_-/A_+|^2$. Results are shown in Fig. 3(a) as a function of the roton energy for two values of q_x (0.7 and 0.8 Å^{-1}). The error bars are mainly due to the fact that the atom wave function is not exactly vanishing, even for the best resonant states resulting from the numerical solution of the equations of motion. This produces a statistical uncertainty in the values of the branching ratio.

Clearly the determination of the reflection coefficient, as well as of the other elements of the scattering matrix, requires the analysis of nonresonant states. In Fig. 3(b) we show our results for the evaporation probabilities and for the reflection coefficient as a function of energy. The numerical uncertainty on these values is expected to be less than 10%. The analysis allows us to estimate also the probability P^{+-} for the roton change-mode reflection, $R^+ \leftrightarrow R^-$. We obtain $P^{+-} \simeq 0.3$ and 0.2 at $\hbar\omega = 10.8$ and 11.3 K, respectively.

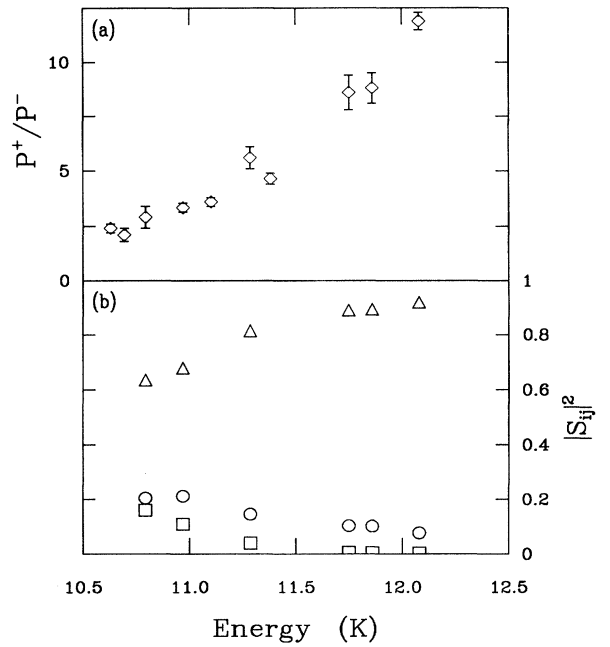

FIG. 3. Ratio of the P^+ and P^- evaporation probabilities (top) and absolute values of the evaporation and reflection probabilities (bottom) as a function of energy. Triangles, circles, and squares correspond to P^+, P^-, and R, respectively. All values below 11.5 K are calculated at fixed parallel wave vector $q_x = 0.7$ Å^{-1}, the others at $q_x = 0.8$ Å^{-1}.

The main conclusions emerging from our results are as follows: (i) Quantum effects give rise to sizable evaporation rates of rotons in the region of energy and angles where evaporation is not allowed classically. (ii) R^- rotons turn out to be less active in the evaporation process than R^+ rotons. (iii) The probability for the roton change-mode reflection is sizable in the energy interval considered and decreases with energy. (iv) The atom reflection coefficient is smaller than 10% for energy greater than about 11 K, and decreases for higher energies.

The remarkable asymmetry between P^+ and P^- at high energy is consistent with the fact that approaching the maxon energy one expects $P^- \longrightarrow 0$. Evaporation from R^+ rotons becomes dominant when the energy increases. The value of the reflection coefficient below 11 K is still too large with respect to the experimental data [15], but nevertheless its sizable decrease from the classical value $R = 1$ reveals the very important role played by quantum effects. The remaining discrepancy with experiments is likely associated with inelastic processes not accounted for in the present calculation.

The above results concern the region of large q_x and large incident angles, where phonons do not take part in the process. For normal impact and energy smaller than the roton minimum (but larger than 7.15 K), one has the opposite regime, where only phonons take part in the scattering process. The results of our calculations in this case give very small values for the atom reflection coefficient, in agreement with experiments.

We are indebted to C. Carraro and A. F. G. Wyatt for many fruitful discussions. This work was partially supported by the U.S. Department of Energy Office of Basic Sciences under Contract No. W-31-109-ENG-38.

[1] M. Brown and A. F. G. Wyatt, J. Phys. Condens. Matter **2**, 5025 (1990).
[2] W. D. Johnston and J. G. King, Phys. Rev. Lett. **16**, 1191 (1966).
[3] S. Balibar, J. Buechner, B. Castaing, C. Laroche, and A. Libchaber, Phys. Rev. B **18**, 3096 (1978).
[4] M. J. Baird, F. R. Hope, and A. F. G. Wyatt, Nature (London) **304**, 325 (1983); F. R. Hope, M. J. Baird, and A. F. G. Wyatt, Phys. Rev. Lett. **52**, 1528 (1984).
[5] A. F. G. Wyatt, Physica (Amsterdam) **126B**, 392 (1984).
[6] G. M. Wyborn and A. F. G. Wyatt, Phys. Rev. Lett. **65**, 345 (1990).
[7] H. Baddar, D. O. Edwards, T. M. Levin, and M. S. Pettersen, Physica (Amsterdam) **194–196B**, 513 (1994).
[8] C. Enss, S. R. Bandler, R. E. Lanou, H. J. Maris, T. More, F. S. Porter, and G. M. Seidel, Physica (Amsterdam) **194–196B**, 515 (1994).
[9] A. Widom, Phys. Lett. **29A**, 96 (1969); D. S. Hyman, M. O. Scully, and A. Widom, Phys. Rev. **186**, 231 (1969).
[10] P. W. Anderson, Phys. Lett. **29A**, 563 (1969).
[11] M. W. Cole, Phys. Rev. Lett. **28**, 1622 (1972).
[12] C. Caroli, B. Roulet, and D. Saint-James, Phys. Rev. B **13**, 3875 (1976); **13**, 3884 (1976).
[13] H. J. Maris, J. Low Temp. Phys. **87**, 773 (1992).
[14] P. A. Mulheran and J. C. Inkson, Phys. Rev. B **46**, 5454 (1992).
[15] D. O. Edwards, Physica (Amsterdam) **109 & 110B**, 1531 (1982), and references therein; V. V. Nayak, D. O. Edwards, and N. Masuhara, Phys. Rev. Lett. **50**, 990 (1983); S. Mukherjee, D. Candela, D. O. Edwards, and S. Kumar, Jpn. J. Appl. Phys. **26-3**, 257 (1987); A. F. G. Wyatt *et al.* (unpublished).
[16] A. F. G. Wyatt, M. A. H. Tucker, and R. F. Cregan, Phys. Rev. Lett. **74**, 5236 (1995).
[17] A. Lastri, F. Dalfovo, L. Pitaevski, and S. Stringari, J. Low Temp. Phys. **98**, 227 (1995).
[18] Actually experimental data show significant reflection only when the perpendicular component q_z of the atom wave vector is close to zero. The threshold behavior of the reflection coefficient has been also discussed in D. P. Clogherty and W. Kohn, Phys. Rev. B **46**, 4921 (1992), in the general context of the quantum theory of sticking.
[19] F. Dalfovo, A. Lastri, L. Pricaupenko, S. Stringari, and J. Treiner, Phys. Rev. B **52**, 1193 (1995).
[20] S. T. Beliaev, Zh. Eksp. Teor. Fiz. **34**, 417 (1958) [Sov. Phys. JETP **7**, 289 (1958)].